MOTOR CONTROL OF A LIMB SEGMENT ACTUATED BY ARTIFICIAL MUSCLES

S. Eskiizmirliler[1, 3], B. Tondu[2], C. Darlot[3]

[1]AASS, Department of Technology, Örebro University, Örebro, Sweden
[2]Department of Electrical and Computer Engineering, INSA, Toulouse, France
[3]Department of Signal and Image Processing, ENST, Paris, France

Abstract-**In this article we present a biologically inspired motor control scheme based on sensory-motor interaction modalities within the Central Nervous System, and its application to the control of a single joint limb segment actuated by two pneumatic McKibben muscles. The embedded Artificial Neural Network (ANN) module's architecture, whose functioning is regulated by reinforcement learning, is similar to the connectivity of cerebellar cortex. Various biologically plausible learning schemes, which enable functional plasticity in the cerebellar cortex, are discussed. The simulation and experimental results are then reported.**
Keywords - **Motor control, brain models, artificial neural networks, reinforcement learning, artificial muscles.**

I. INTRODUCTION

This article addresses the problem of how the cerebellum processes premotor orders so that the fast movements, which have a shorter duration than the sum of the transmission and processing delays in the motor and sensory pathways, can be accurate. By definition, fast movements cannot be regulated in closed-loop using the sensory signals, but must be driven in open-loop, by motor orders that must be computed as the movement proceeds and take into account the dynamical and geometrical characteristics of the limb to be moved. This can be mathematically stated as the problem of inverting the bio-mechanical function of the limb.

In previous articles [1,2,3], we presented a circuit that allows estimation of an inverse function by avoiding an explicit inversion operation. The model was first tested by simulations of eye and forearm movements [4]. According to an anatomical interpretation, the predictive elements of the model would be embedded in the cerebellar cortex, and the function of the whole Cerebellum would be to compute approximate inversions. Therefore, the second step consisted of replacing the elements which are interpreted as parts of the cerebellar cortex by an ANN architecture whose blueprint is copied from the well-known connectivity of the cerebellar cortex [5,6].

The present work is intended first to equip the model with a circuit that would represent the inferior olive and then to apply various learning mechanisms that differ from each other with the inclusion of different parts of the cerebellar cortex in the calculation of an error signal on the inferior olive. A single joint robot limb actuated by two artificial McKibben pneumatic muscles [7] was chosen to mimic the human forearm movements. The expanded model was trained until the desired movement was accurately performed both by the simulations and by replacing the peripheral part with the real robot limb in order to realize real time learning [8,9].

II. MODEL OF MOTOR CONTROL

A. General circuit

The general circuit is shown in Fig. 1A. Blocks noted g_1 and g_2 represent the bio-mechanical functions of two antagonist muscles actuating a limb segment whose dynamics is represented by G. The elements encircled with a rectangle drawn in dashed lines are interpreted as representing the cerebellar cortex which would be able to compute the estimates g^*, G^* of kinematic variables g and G before the movement is launched but after the motor transmission delays D_1 and D_2. The summing elements from which issue Q_1 and Q_2 are interpreted as representing the cerebellar nuclei. The regulating pathways via the Inferior Olive are drawn here in dashed lines to recall that no learning takes place in the initial cybernetic circuit. The input signal being the premotor velocity profile $\dot{\Theta}^D$ of the desired movement, this circuit is able to compute the actual position Θ^A [4].
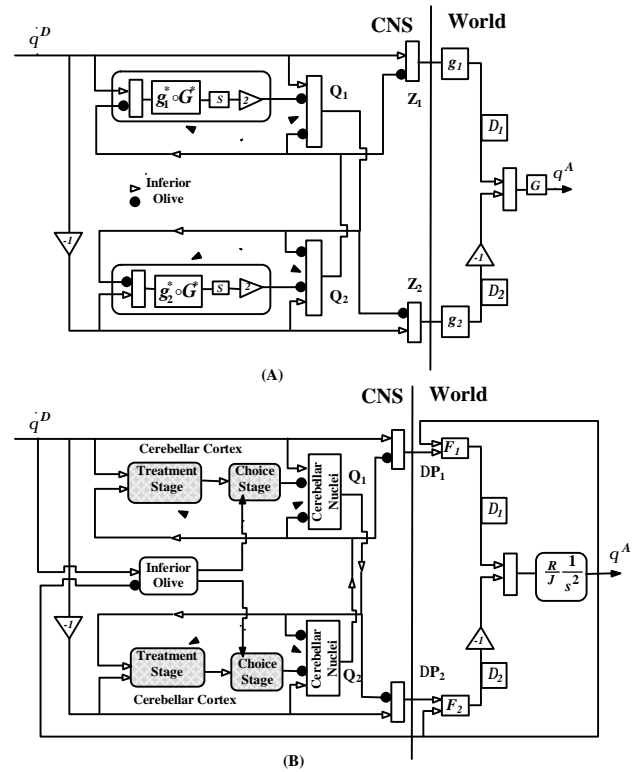

(A)

(B)

Fig.1. Cybernetic circuits proposed for motor control of two antagonist muscles. Empty arrows represent positive (excitatory) connections and black dots negative (inhibitory) connections. (A) The initial cybernetic circuit, (B) the circuit equipped by the ANN architecture and the Inferior Olive.

Report Documentation Page

Report Date	Report Type	Dates Covered (from... to)
25OCT2001	N/A	-

Title and Subtitle	Contract Number
Motor Control of a Limb Segment Actuated by Artificial Muscles	Grant Number
	Program Element Number

Author(s)	Project Number
	Task Number
	Work Unit Number

Performing Organization Name(s) and Address(es)	Performing Organization Report Number
AASS, Department of Technology, Örebro University, Örebro, Sweden	

Sponsoring/Monitoring Agency Name(s) and Address(es)	Sponsor/Monitor's Acronym(s)
US Army Research, Development & Standardization Group (UK) PSC 802 Box 15 FPO AE 09499-1500	Sponsor/Monitor's Report Number(s)

Distribution/Availability Statement
Approved for public release, distribution unlimited

Supplementary Notes
Papers from the 23rd Annual International Conference of the IEEE Engineering in Medicine and Biology Society, 25-28 Oct 2001, held in Istanbul, Turkey. See also ADM001351 for entire conference on cd-rom., The original document contains color images.

Abstract

Subject Terms

Report Classification	Classification of this page
unclassified	unclassified

Classification of Abstract	Limitation of Abstract
unclassified	UU

Number of Pages
4

B. Embedding the ANN in the control circuit

Fig. 1B represents a modified version of the initial circuit having the learning ability thanks to the embedded ANN. For the sake of biological plausibility, the architecture of the ANN representing the cerebellar cortex was chosen to be similar to the anatomical connectivity [5] as shown in Fig. 2.
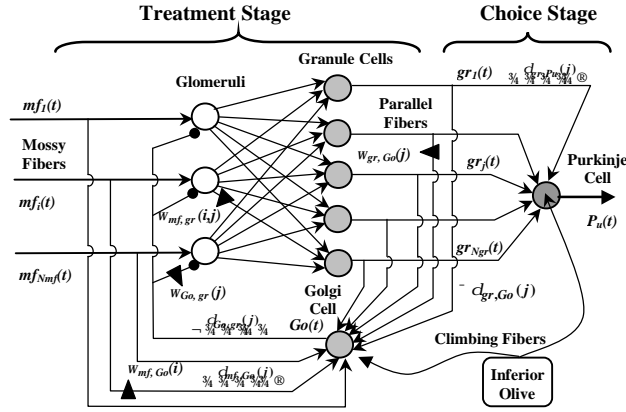
Fig.2. The ANN's architecture representing the cerebellar cortex. Adaptive weights are noted ω and symbolized by black triangles while the transmission delays are noted δ. Stellate and Basket cells are not represented and the ratios of various cell types were not respected.

This ANN whose functioning is detailed in [8,9] is expected to learn how to estimate an internal representation of the peripheral part's dynamics (i.e. the experimental apparatus), under supervision of a teaching signal.

C. Learning driven by a teaching signal issued from inferior olive

According to the proposed anatomical interpretation, this signal would represent climbing fiber activity issued from the inferior olive which is modeled in this work as shown in Fig.3 to detect over- or under-shoots of movements and correct ongoing movements. The teaching signal sent to the neural network (Fig. 2) is a square pulse of fixed unit amplitude and of 5 ms duration, which thus did not encode the amplitude of the error.
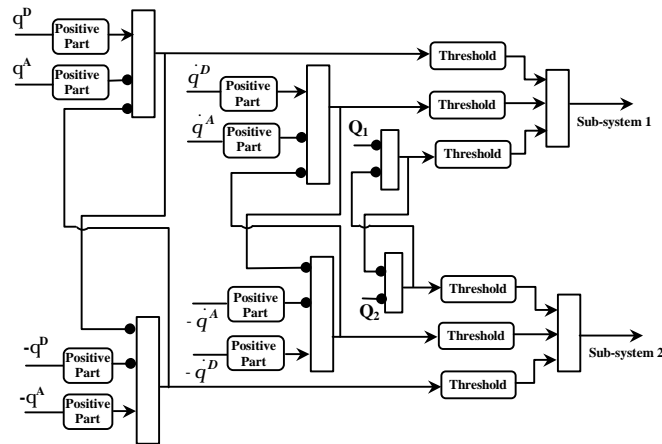
Fig.3. Circuit representing the inferior olive.

To keep information about synapse activity during the movement (credit assignment problem), a synaptic *eligibility* is calculated by a first-order low-pass filter as in (1).

$$t_i \frac{de_i}{dt} + e_i(t) = gr_i(t) \qquad (1)$$

Then the learning rule becomes:

$$\Delta w_{gr,P}(i) = -h \cdot FG(t) \cdot e_i(t) \qquad (2)$$

where **h** is a small and positive learning rate and FG(t) is the teaching signal carried by the climbing fibers and calculated according to the four following conditions:

- **Condition A:** The error calculation takes only into account the difference between the desired and achieved final positions.

- **Condition B:** The error calculation takes into account both the differences in position and in velocity. To represent the intermittent control by the inferior olive, the teaching signal was kept silent during a latency delay of 400 ms after each launch of the arm.

- **Condition C:** The error calculation is similar to that of condition B, and in addition the short-term reduction in Purkinje cell activity following the firing of the climbing fiber is also taken into account. The amplitude of the ANN's output signal is multiplied by 0.9 during the first 30 ms after the occurrence of the teaching signal.

- **Condition D:** The error calculation is similar to that of condition C, and in addition the values of the signals **Q** issued from the summing elements interpreted as the cerebellar nuclei are reduced. This was aimed at coarsely modeling minimization of energy expenditure, since signals **Q** encode partly the forces to be exerted by the muscles. A teaching signal was applied whenever the values of **Q** exceeded a threshold empirically set, after several trials, to a value of 10 (arbitrary units).

D. Actuator of two antagonistic McKibben muscles

An artificial McKibben pneumatic muscle, consisting of a braided shell surrounding a rubber inner tube, is defined by its length (l_0), mean radius (r_0) and braid angle (α_0) when it is not under pressure. When compressed air is blown in, the muscle contracts to generate an axial contraction force which can be described in terms of the contraction rate (ε) [7]. The initial circuit was finally modified so as to drive the experimental apparatus shown in Fig.4 which consists of a mechanical segment actuated by two artificial McKibben muscles whose dynamic behavior can be represented by (3) and the values reported in Table 1.
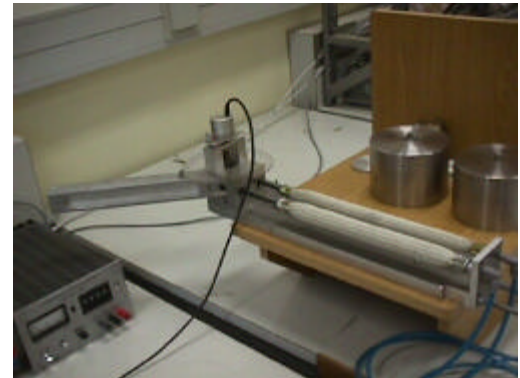
Fig.4. Experimental apparatus with two McKibben muscles.

$$J.\frac{d^2\Theta}{dt^2} = 9.81.R\left[F_1 - F_2\right]$$

where:

(3)

$$F_1 = f_{max}\left(P_0 + \Delta P_1\right)\left[1 - \frac{1}{\epsilon_{max}}\left(\epsilon_0 + \frac{R\Theta}{l_0}\right) - C\frac{R}{l_0}\frac{d\Theta}{dt}\right]$$

$$F_2 = f_{max}\left(P_0 - \Delta P_2\right)\left[1 - \frac{1}{\epsilon_{max}}\left(\epsilon_0 - \frac{R\Theta}{l_0}\right) + C\frac{R}{l_0}\frac{d\Theta}{dt}\right]$$

J = Moment of inertia of the rod

R = Radius of the pulley

Θ = Angular position counted from the rest position

Po = Initial air pressure

ΔPᵢ = Air pressure difference

C = Coefficient of the viscosity

Table 1: Simulation values

Parameter	Value	Parameter	Value
l_0	0.3m	P_0	2.5 bars
R	0.015m	ϵ_0	0.1
J	0.05 kg.m^2	ϵ_{max}	0.25
C	500 N.s	f_{max}	20 kgf/bars

III. RESULTS

The training of the model was performed in two ways. First the forearm movements were simulated by replacing the peripheral system with the model of the robot limb segment shown in Fig. 4. Then, the experimental apparatus was used to mimic by itself the same movements. The results obtained by performing four different learning schemes, A to D, in either ways are shown in Fig. 5 and Fig. 6 respectively.
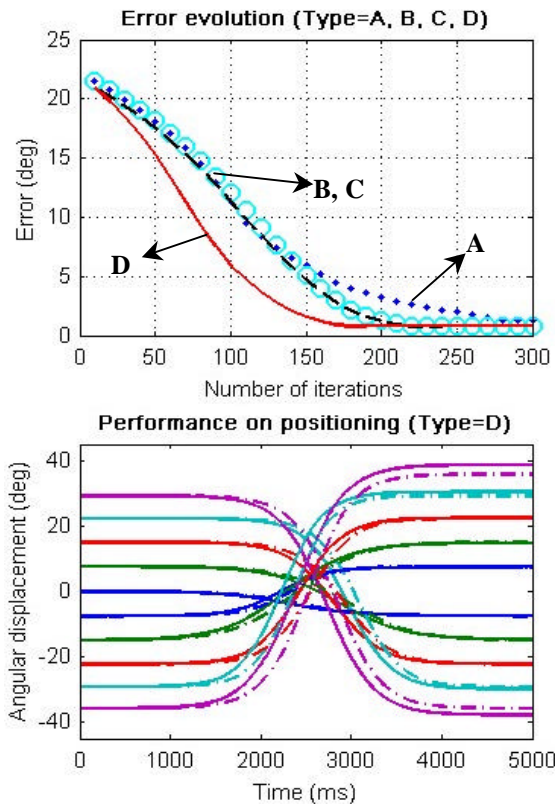

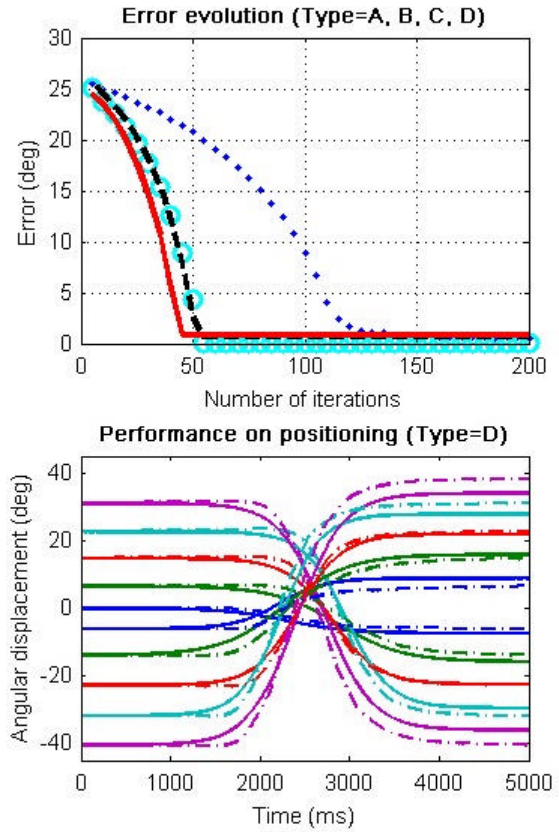Fig. 5. Model's learning capacity on simulated robot limb movements.

Fig. 6. Model's learning capacity on real robot limb movements.

Curves on the top of the Fig. 5 and 6 show the evolution of the mean squared error as learning proceeds, while the curves on the bottom show the results of the set of 10 movements performed after learning of type D. Solid and dashed lines represent respectively desired and actual movements. The ANN was composed of twenty granular cells with time constants randomly set in the range 1-6 ms, one Golgi cell and one Purkinje cell with time constants of 10 ms. Transmission delays δ between cells were randomly set in the range 1-10 ms. The motor delays Δ_1 and Δ_2 were set to 50 ms. The learning phase proceeded in 300 iterations on a predefined set of 5 positive (counterclockwise) and 5 negative (clockwise) horizontal movements, each being presented alternately at a time. Each movement lasted 5 seconds and all velocity profiles were centered on 2.5s. The amplitude range was ± 40 degrees.

The change in the calculation of the teaching signal considerably affects the number of iterations needed for achieving the desired movement and the best result is obtained with a learning scheme of type D in both testing cases. Some internal signals measured on different sides of the circuits numbered respectively 1 and 2 during two movements of same amplitude but with different velocities are illustrated in figures 7 and 8. On each figure, from left to right and from top to bottom, the curves in the rectangles show desired (dashed lines) and achieved (solid lines) angular displacements, time-courses of signals issued from Purkinje cells, motor orders and finally the force profiles measured by force sensors.
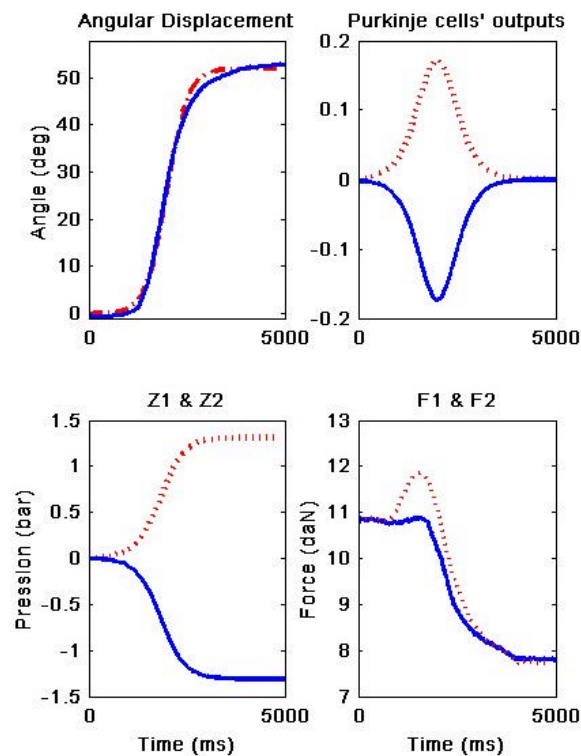
Fig. 7. Internal signals, during a slow movement. Except for the top right corner, the curves plotted in dotted and solid lines represent the signals measured on side 1 and 2 of the circuit shown in Fig.1B respectively.
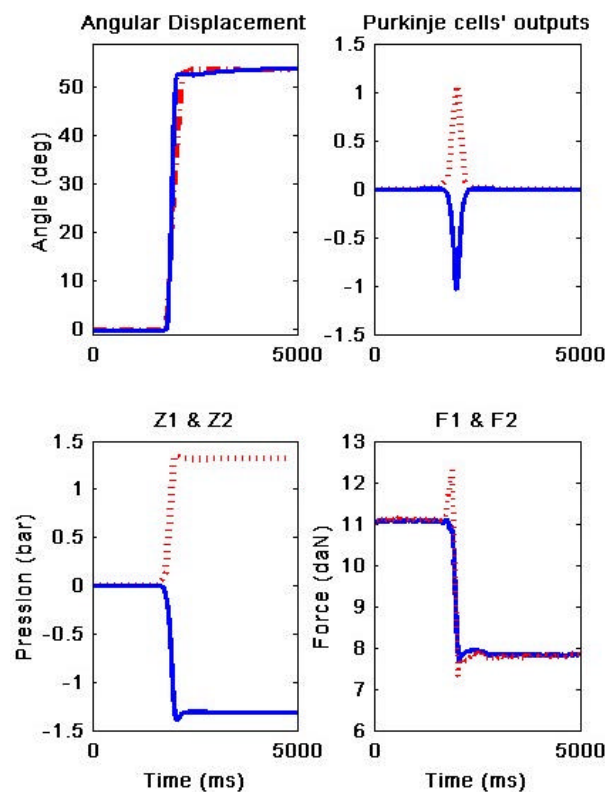

Fig. 8. Internal signals during a fast movement. Except for the top right corner, the curves plotted in dotted and solid lines represent the signals measured on side 1 and 2 of the circuit shown in Fig.1B respectively.

IV. CONCLUSIONS

This model of the cerebellar pathways, although quite simplified, suffices to control movements of a single segment, actuated by means of artificial muscles endowed with non-linear characteristics. Its connectivity accounts essentially for the divergence of information carried by the mossy fibers to the granule cells and then the convergence of the latters' outputs conveyed by parallel fibers within the dendritic arborizations of the Purkinje cells. After learning, the output signal of the ANN (i.e. Purkinje cells whose axons convey the output signal of the cerebellar cortex to the cerebellar nuclei) anticipates the velocity of the movement achieved by the mobile segment. As a consequence, the motor orders which result from the addition of the various premotor orders in the motoneurons can be considered as encoding a "virtual trajectory", which is not calculated on purpose since it results from the functioning of feedback loops consistent with anatomy and assumed to be internal to the CNS.

Altogether, the looped structure and the anticipative ability allow both the model to invert the bio-mechanical functions and to integrate the premotor velocity signals. Notably, movements of the same amplitude can be driven at different velocities, and the time-courses of the forces exerted by the pneumatic muscles resemble those of the electromyograms of real muscles during arm movements at various velocities. Thus, the merging of an ANN designed to account for cell connectivity in a cybernetic model grounded on functional principles, enables both the control of a simple robot and reproduction of physiological observations.

REFERENCES

[1] J. Droulez and C. Darlot, "The geometric and dynamic implications of the coherence constraints in three-dimensional sensorimotor interactions," in: Attention and Performance XIII, Jeannerod M, Eds, Lawrence Erlbaum, Hillsdade, 1989, pp. 495-526.

[2] C. Darlot, "The cerebellum as a predictor of neural messages. I. The stable estimator hypothesis," *Neuroscience*, vol. 56, pp. 617-646, 1993.

[3] P. Denise and C. Darlot, "The cerebellum as a predictor of neural messages. II. Role in motor control and motion sickness," *Neuroscience,* vol. 56, pp. 647-655, 1993.

[4] C. Darlot, L. Zupan, O. Etard, P. Denise and A. Maruani, " Computation of inverse dynamics for the control of movements," *Biol. Cybern.,* vol. 75, pp. 173-186, 1996.

[6] N. Schweighofer, M.A. Arbib, P.F. Dominey, "A model of the cerebellum in adaptive control of saccadic gain. 2- Simulation results," *Biol. Cybern.*, vol. 75, pp. 29-36, 1996.

[7] B. Tondu, P. Lopez, "Modeling and control of McKibben artificial muscle robot actuators", IEEE Control Systems, vol. 20/2, pp. 15-38, 2000.

[8] S. Eskiizmirliler, " Modelling of sensory-motor information fusion in the cerebellar pathways. Application to the motion sickness in high speed tilting trains, and to the control of robot limb actuated by 2 artificial muscles," Ph.D. Thesis, Ecole Nationale Supérieure des Télécommunications, Paris, 2000.

[9] S. Eskiizmirliler, N. Forestier, B. Tondu, C. Darlot, " A model of cerebellar pathways applied to the control of a mobile mechanical segment", *Biol. Cybern.*, 2001, in press.